Lipids in Health and Disease

RESEARCH

Open Access

Gender-specific correlations between serum lipid profiles and intra-pancreatic fat deposition: a cross-sectional study

Ting Ran[1,2†], Yanni Wang[1,2†], Fengxi Yuan[1,2], Ruoyi Liu[1], Meng Ye[1], Miao Zhang[1], Xia Du[3*] and Jing Zheng[1*]

Abstract

Background Intra-pancreatic fat deposition (IPFD) is linked to metabolic and pancreatic diseases. MRI, while precise, is not cost-effective for routine IPFD screening, highlighting the need for accessible biomarkers. This study aims to analyze the relationships among serum lipid profiles, lipoprotein ratios, and IPFD, with a focus on sex differences.

Methods Data from adults at the Affiliated Hospital of Guizhou Medical University between 2018 and 2019 were analyzed. The subjects underwent routine Siemens 64-slice spiral CT scans, and IPFD was quantified via a quantitative computed tomography post-processing station. Lipid panel components were analyzed in the fasted state. Linear regression models stratified by gender were applied to evaluate these associations.

Results The study included 1,046 participants after exclusions, with significant sex differences found in the correlations between serum lipids, lipoprotein ratios, and IPFD. In females, remnant cholesterol was strongly associated with total IPFD (R2 = 0.155, $P < 0.001$), and similarly strong correlations existed with fat deposition in the pancreatic head ($R^2 = 0.124$, $P = 0.003$), body ($R^2 = 0.102$, $P = 0.001$), and tail ($R^2 = 0.146$, $P = 0.005$). Total cholesterol was also positively correlated with IPFD in females, particularly with the total IPFD ($R^2 = 0.145$, $P = 0.002$) and IPFD in the pancreatic head ($R^2 = 0.177$, $P = 0.003$) and body ($R^2 = 0.100$, $P = 0.001$). In males, triglycerides were notably correlated with IPFD in the tail ($R^2 = 0.200$, $P = 0.045$), but not in other regions. Similarly, total cholesterol was correlated with IPFD in the tail ($R^2 = 0.197$, $P = 0.041$). Additionally, in males, the triglyceride/high-density lipoprotein cholesterol ratio showed a positive association with tail fat deposition ($R^2 = 0.200$, $P = 0.033$).

Conclusion Significant differences between genders were evident in the correlations of serum lipids and lipoprotein ratios with IPFD. In women, remnant cholesterol was strongly correlated with IPFD, suggesting its potential as a biomarker.

Keywords Serum lipid profiles, Lipoprotein Ratios, Intra-pancreatic Fat Deposition

†Ting Ran and Yanni Wang contributed equally to this work.

*Correspondence:
Xia Du
12132950@qq.com
Jing Zheng
Ava1223@163.com

[1]Department of Endocrinology, The Affiliated Hospital of Guizhou Medical University, No. 28 Guiyi Street, Guiyang 550004, China
[2]Guizhou Medical University, Guiyang 550004, China
[3]Department of Radiology, The Affiliated Hospital of Guizhou Medical University, Guiyang 550004, China

Introduction

Over the past decade, intra-pancreatic fat deposition (IPFD) has garnered significant research interest and is now recognized as a critical ectopic fat characteristic linked to the rising incidence of metabolic and pancreatic disorders [1]. IPFD is linked to, at minimum, a two-fold increase in diabetes risk [2]. Moreover, IPFD plays a pivotal role in developing pancreatic exocrine diseases, encompassing pancreatic tumors, acute pancreatitis, and chronic pancreatitis, along with their consequences, such as pancreatic exocrine insufficiency and diabetes exocrine pancreatic (DEP) [3–5]. Various imaging methods, such as ultrasound, CT, and MRI, are routinely employed to assess IPFD. Conventional ultrasound is widely accessible but can only provide a semiquantitative analysis, and its effectiveness is hindered by the retroperitoneal position of the pancreas and intestinal gas [6]. MRI is the most accurate method for quantifying IPFD but is time-consuming and costly [7, 8]. CT is reliable and accurate but involves significant radiation exposure [9]. Thus, there is a pressing need to develop cost-effective, precise, and easily accessible blood-based biomarkers for IPFD to enable early detection of high-risk individuals.

The serum lipid is among the commonly acquired set of blood parameters in routine clinical practice. A 2017 systematic review of IPFD biomarkers revealed correlations between IPFD and lipid metabolism markers, including low-density lipoprotein cholesterol (LDL-C), high-density lipoprotein cholesterol (HDL-C), and triglycerides (TG) [10]. Total cholesterol (TC) was examined in relation to IPFD in five studies [11–15]. Remnant cholesterol (RC) has come under focus due to its link with cardiovascular disease, with Skudder-Hill et al. [16] finding a notable correlation between RC and IPFD. Serum protein ratios such as TG/HDL-C and TC/HDL-C are strongly linked to insulin resistance [14, 17], which was linked to intra-pancreatic fat deposition by Patel et al. [18]. These results indicate a possible link between the serum lipoprotein ratio and IPFD.

Nadarajah et al. [19] studied the relationship between pancreatic fat deposits in different sites with T2DM and showed that increased fat deposits in the tail of the pancreas identified patients at risk for T2DM. This indicates that fat deposition in different regions of the pancreas might have distinct effects.

Most previous studies focused on the relationship between lipid profiles and total IPFD and did not explore potential sex differences in these associations. Therefore, the aim of this study was to investigate the relationships between serum lipid profiles, lipoprotein ratios, and fat deposition in different regions of the pancreas, with a specific focus on sex-based differences.

Methods

Object of study

Participants were adults who underwent abdominal CT scans during the 2018–2019 physical examination cohort in the Affiliated Hospital of Guizhou Medical University. The exclusion criteria included chronic liver disease; acute or chronic pancreatitis; prior weight loss surgery; malignancy; the use of medications affecting body weight or metabolism; engagement in dieting, exercise, or weight-loss medications in the preceding 6 months; pregnancy or lactation; and contraindications to quantitative computed tomography (QCT), such as implants, metals, or other foreign objects at the measurement site.

Measurements

All measurements in this research were performed by skilled nurses. Human body measurement data, including height (cm), weight (kg), diastolic blood pressure (mmHg), and systolic blood pressure (mmHg), were accurate to one decimal place. Weight and height were used to calculate body mass index (BMI).

QCT imaging technique

The subjects underwent routine upper abdomen CT scans using a Siemens SOMATOM Definition AS+64-row spiral CT scanner with a Mindways QCT phantom (CT calibration phantom). Prior to scanning, the subjects fasted for 4–6 h, were provided with water, remained conscious, and received training. During the scans, the subjects were supine and held their breath to complete the scan in one position. The scan settings included a bed height of 135 cm, a pitch of 0.5, a tube voltage of 120 kV, a current of 200 mA, a fixed milliampere-second, a tube rotation speed of 0.5/s/circle, a scan pitch of 0.5, a default window set to 400 HU in width and positioned at 40 HU for the original image, and detector collimation of 128×0.6 mm. After the scan was complete, the raw abdominal CT data were reconstructed using the B30f medium smooth soft tissue algorithm. An image using thin layer reconstruction with a thin layer of 1 mm thickness, 1 mm spacing, and a DFOV of 500 mm was uploaded to the QCT post-processing workstation via a Siemens film reading workstation from Germany. Next, mapping the pancreas's region of interest (ROI). First, the pancreas was divided into three parts using the superior mesenteric vein as an anatomical landmark. The pancreatic head region was defined as the pancreatic tissue located to the right-hand side of the superior mesenteric vein, near the duodenal bulb. The pancreatic body and tail were distinguished by dividing the pancreatic tissue on the left side of the superior mesenteric vein into two equal parts, with the portion closer to the spleen designated as the pancreatic tail and the remainder designated as the pancreatic body [20]. Subsequently, the pancreatic

BMD was assessed using the lumbar spine method, with ROIs positioned over the pancreatic head, body, and tail, excluding surrounding tissues. Each ROI was 100–140 mm^2, with an average of three measurements per region. To quantitatively measure liver fat, ROIs were set up on the section where the liver is entered by the right branch of the portal vein. Three circular ROIs were plotted on the left, right anterior, and right posterior lobes, covering an area of approximately 243 square millimeters. Clear avoidance of prominent blood vessels and bile ducts was maintained. The field homogeneity correction value, associated BMD values, and calibration slope from three assessments in the QCT Pro software database were exported. The measurement data were independently collected by two experienced radiologists (Fig. 1). QCT assessments of liver and pancreatic tissue, acquired using the Mindways spinal module software, were converted into fat percentage values using the method by Xiaoguang Cheng et al., following Eqs. [21–23]:

$$\%\mathrm{fat}_{\mathrm{pancreas}} = \left(\frac{\mathrm{Hu}_{\mathrm{leanpancreas}} - \mathrm{Hu}_{\mathrm{pancreas}}}{\mathrm{Hu}_{\mathrm{leanpancreas}} - \mathrm{Hu}_{\mathrm{fat}}}\right) \times 100\%$$

$$\%\mathrm{fat}_{\mathrm{liver}} = \frac{\mathrm{Hu}_{\mathrm{leanliver}} - \mathrm{Hu}_{\mathrm{liver}}}{\mathrm{Hu}_{\mathrm{leanliver}} - \mathrm{Hu}_{\mathrm{fat}}} \times 100\%$$

The HU_{liver} and $HU_{pancreas}$ represent the radiodensity measurements within the hepatic and pancreatic ROIs, which were transformed from bone mineral density (BMD) readings into radiodensity metrics using Mindways QCT Pro calibration. HU_{fat}, $HU_{lean\ liver}$, and $HU_{lean\ pancreas}$ represent, respectively, the attenuation measurements for 100% fat, lipid-free hepatic tissue, and lipid-free pancreatic tissue. Their values were calculated based on the base set equivalent densities of dipotassium hydrogen phosphate (K2HPO4) and water for adipose and fat-free tissues and using scan calibration data from the QCT Pro software to adjust for tube voltages and differences in beam hardening from person-to-person.

The Tissue Composition Module in QCT Pro was used to image the cross-sectional level of the L2/L3 intervertebral space, and automatically calculated the SAT and VAT areas (cm^2) after thresholds were set with AutoSnake.

Laboratory measurements

The participants underwent an 8–10 h fast before their blood was sampled. TG, TC, LDL-C, and HDL-C were assessed using a Roche Cobas 8000 analyzer, and RC was calculated as RC=TC–HDL-C–LDL-C [24]. Fasting plasma glucose was assessed via a hexokinase colorimetric assay.

Statistical analyses

Parameters exhibiting near-normal or normal distributions were represented as the average ± standard deviation (X ± SD). Non-normally distributed data were characterized as the interquartile range and median (IQR/median). Initial characteristics were compared between male and female participants using the Mann-Whitney U test for continuous variables. Linear regression analysis was used to assess the impact of serum lipid profiles and lipoprotein ratios on IPFD, with findings reported as R^2 values, β coefficients, standard errors, and *P* values. The analyses included three parity categories: Model I, an unadjusted model; Model II, adjusted for age, BMI, and fasting blood glucose; and Model III, which included Model II adjustments and additional adjustments for diastolic and systolic blood pressures and fat deposition in the visceral, subcutaneous, and liver regions. All the statistical evaluations were performed using SPSS version 25.0, with the significance threshold set at $P<0.05$.

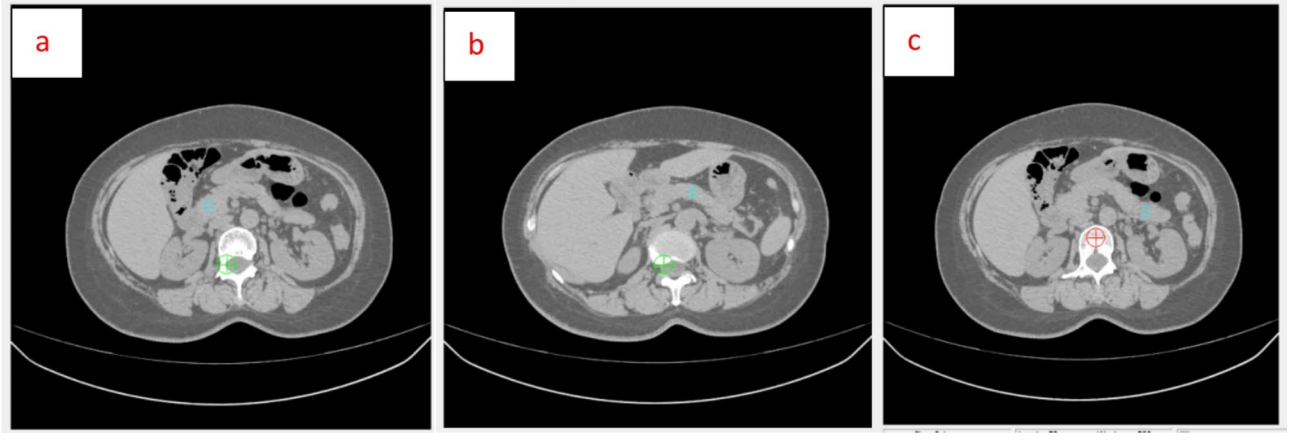

Fig. 1 QCT measurement of pancreatic fat. In **a**, the area circled in blue represents the ROI for the pancreatic head; in **b**, the area circled in blue represents the ROI for the pancreatic body; in **c**, the area circled in blue represents the ROI for the pancreatic tail

Results

Baseline characteristics

The initial cohort consisted of 1,620 participants meeting the eligibility criteria, with 574 excluded because of incomplete lipid panel data. Among the remaining 1,046 participants, 671 were male and 375 were female. Both groups averaged 50 years of age and had similar levels of LDL-C, TC, subcutaneous fat, and fat deposition in the pancreatic body and tail. Compared with women, men had a significantly greater BMI, fasting glucose level, TG level, RC level, TC/HDL-C ratio, visceral fat area, liver fat deposition ($P<0.001$), as well as systolic pressure ($P=0.029$), diastolic pressure ($P=0.030$), total intra-pancreatic fat deposition ($P=0.022$), and intra-pancreatic head fat deposition ($P=0.007$). Conversely, women had higher HDL-C levels ($P<0.001$) and TG/HDL-C ratios ($P<0.001$) (Table 1).

Associations between serum lipid profiles and serum lipoprotein ratios with IPFD in males

In the male cohort, no meaningful associations were observed between TG and total IPFD or fat deposition in the pancreatic head or body in the final adjusted model. However, TG exhibited a positive correlation with IPFD in the tail across all models (Model I: $R^2=0.027$, $P<0.001$; Model II: $R^2=0.095$, $P=0.002$; Model III: $R^2=0.200$, $P=0.045$). TC showed no significant association with total IPFD or fat deposition in the pancreatic body. A significant interaction between TC and fat deposition in the pancreatic head was observed in Model I, although this association was not significant in Models II and III. However, TC exhibited a positive correlation with fat deposition in the pancreatic tail across all models (Model I: $R^2=0.008$, $P=0.007$; Model II: $R^2=0.087$, $P=0.034$; Model III: $R^2=0.197$, $P=0.041$). When exploring the TG/HDL-C ratio link to IPFD, similar results were observed. The TG/HDL-C ratio did not show a significant link with total IPFD or fat deposition in the pancreatic head, or body in the final model, although it exhibited a positive correlation with fat deposition in the pancreatic tail across all models (Model I: $R^2=0.024$, $P<0.001$; Model II: R2=0.095, $P=0.002$; Model III: R2=0.200, $P=0.033$). RC showed no significant correlation with total IPFD or fat deposition in the pancreatic head, body, or tail in the final model. Similarly, the TC/HDL-C ratio showed no significant association with the total IPFD or fat deposition in the head, body, or tail of the pancreas in the final model. Finally, LDL-C showed no significant correlation with total IPFD, or with fat deposition in the pancreatic head, body, or tail across all models (Table 2).

Associations of serum lipid profiles and serum lipoprotein ratios with IPFD in females

In the female cohort, TC was consistently associated with IPFD in all models (Model I: $R^2=0.030$, $P=0.001$; Model II: $R^2=0.049$, $P=0.007$; Model III: $R^2=0.145$, $P=0.002$), and with fat deposition in the head (Model I: $R^2=0.026$, $P=0.002$; Model II: $R^2=0.033$, $P=0.007$; Model III: $R^2=0.177$, $P=0.003$) and body of the pancreas (Model I: $R^2=0.032$, $P=0.001$; Model II: $R^2=0.051$, $P=0.002$; Model III: $R^2=0.100$, $P=0.001$). However, no association was found between TC and fat deposition in the pancreatic

Table 1 Participant characteristics

Characteristics	Male($N=671$)	Female($N=375$)	*p*
Age, year	50 ± 13	50 ± 11	0.893
BMI, kg/m2	25.0 ± 3.1	23.9 ± 3.1	**< 0.001**
Fasting plasma glucose, mmol/L	5.69 ± 1.99	5.20 ± 1.50	**< 0.001**
Systolic pressure, mmHg	96 ± 60	87 ± 63	**0.029**
Diastolic pressure, mmHg	59 ± 37	54 ± 39	**0.030**
TG, mmol/L	2.35 ± 1.76	1.64 ± 1.51	**< 0.001**
TC, mmol/L	4.84 ± 1.02	4.90 ± 1.00	0.339
HDL-C, mmol/L	1.16 ± 0.31	1.48 ± 0.40	**< 0.001**
LDL-C, mmol/L	3.01 ± 0.86	3.04 ± 1.03	0.729
RC, mmol/L	0.67 ± 0.81	0.39 ± 0.98	**< 0.001**
TC/HDL-C	4.41 ± 1.52	3.58 ± 1.68	**< 0.001**
TG/HDL-C	1.43 ± 2.40	2.38 ± 2.48	**< 0.001**
Visceral fat area, cm2	182 ± 80	162 ± 76	**< 0.001**
Subcutaneous fat, cm2	106 ± 48	100 ± 46	0.054
Liver fat deposition, %	14 ± 7	12 ± 6	**< 0.001**
Total intra-pancreatic fat deposition, %	7.1 ± 4.6	6.5 ± 4.2	**0.022**
Intra-pancreatic head fat deposition, %	7.0 ± 5.7	6.1 ± 4.9	**0.007**
Intra-pancreatic body fat deposition, %	7.6 ± 6.2	7.0 ± 5.4	0.129
Intra-pancreatic tail fat deposition, %	6.7 ± 4.3	6.3 ± 4.3	0.119

TG, triglycerides; TC, total cholesterol; RC, remnant cholesterol; HDL-C, high-density lipoprotein cholesterol; LDL-C, low-density lipoprotein cholesterol; BMI, body mass index

Table 2 Correlations between serum lipid profiles, serum lipoprotein ratios, and the deposition of fat in the pancreas of males

Component/Model	Total				Head				Body				Tail			
	R2	*β*	SE	*p*	R2	*β*	SE	*p*	R2	*β*	SE	*p*	R2	*β*	SE	*p*
Triglycerides																
Model I	0.021	0.372	0.100	**< 0.001**	0.023	0.490	0.125	**< 0.001**	0.004	0.221	0.139	0.112	0.027	0.403	0.095	**< 0.001**
Model II	0.074	0.259	0.103	0.057	0.078	0.309	9.128	**0.016**	0.018	0.166	0.146	0.255	0.095	0.303	0.097	**0.002**
Model III	0.182	0.126	0.100	0.206	0.188	0.147	0.124	0.236	0.059	0.045	0.148	0.760	0.200	0.188	0.093	**0.045**
Total cholesterol																
Model I	0.005	0.330	0.174	0.059	0.004	0.338	0.218	**0.009**	0.002	0.286	0.239	0.815	0.008	0.381	0.166	**0.007**
Model II	0.070	0.304	0.172	0.077	0.074	0.276	0.214	0.196	0.018	0.303	0.242	0.210	0.087	0.346	0.162	**0.034**
Model III	0.183	0.289	0.169	0.087	0.189	0.254	0.209	0.225	0.061	0.299	0.248	0.229	0.197	0.325	0.159	**0.041**
Remnant cholesterol																
Model I	0.006	0.450	0.218	**0.039**	0.006	0.562	0.272	**0.039**	< 0.001	0.145	0.299	0.628	0.015	0.662	0.207	0.256
Model II	0.067	0.275	0.220	0.212	0.073	0.263	0.273	0.336	0.016	0.063	0.309	0.838	0.089	0.515	0.207	**0.013**
Model III	0.179	0.095	0.211	0.652	0.187	0.045	0.262	0.864	0.058	-0.078	0.31	0.801	0.195	0.337	0.198	0.089
High-density lipoprotein cholesterol																
Model I	0.006	-1.172	0.565	**0.038**	0.010	-1.834	0.703	**0.009**	< 0.001	-0.182	0.776	0.815	0.011	-1.467	0.538	**0.007**
Model II	0.067	-0.630	0.557	0.258	0.075	-1.098	0.691	0.113	0.016	0.168	0.782	0.803	0.084	-0.923	0.527	0.080
Model III	0.179	0.203	0.541	0.708	0.187	-0.089	0.671	0.859	0.060	0.967	0.794	0.224	0.192	-0.239	0.509	0.639
Low-density lipoprotein cholesterol																
Model I	0.001	0.183	0.207	0.377	0.001	0.184	0.259	0.477	0.001	0.248	0.284	0.382	0.001	0.119	0.198	0.548
Model II	0.067	0.239	0.202	0.237	0.073	0.273	0.252	0.278	0.017	0.294	0.284	0.301	0.081	0.150	0.192	0.785
Model III	0.181	0.265	0.199	0.183	0.189	0.307	0.246	0.213	0.060	0.307	0.292	0.294	0.192	0.177	0.187	0.343
Triglycerides/High-density lipoprotein cholesterol																
Model I	0.016	0.234	0.071	**0.001**	0.015	0.278	0.089	**0.002**	0.004	0.150	0.098	0.127	0.024	0.273	0.067	**< 0.001**
Model II	0.072	0.160	0.072	**0.027**	0.075	0.158	0.090	0.079	0.018	0.115	0.102	0.260	0.095	0.208	0.068	**0.002**
Model III	0.181	0.007	0.014	0.625	0.187	0.066	0.087	0.446	0.059	0.045	0.103	0.660	0.200	0.139	0.065	**0.033**
Total Cholesterol/High-density lipoprotein cholesterol																
Model I	0.012	0.326	0.117	**0.005**	0.011	0.395	0.145	**0.007**	0.002	0.193	0.160	**0.047**	0.019	0.391	0.111	**< 0.001**
Model II	0.071	0.225	0.116	0.054	0.075	0.238	0.145	0.100	0.017	0.146	0.164	0.374	0.090	0.290	0.110	0.008
Model III	0.180	0.117	0.112	0.299	0.187	0.112	0.140	0.422	0.058	0.045	0.166	0.786	0.196	0.194	0.106	0.067

Note: Data are presented as R2 values, unstandardized β coefficients, standard errors, and *P* values (from linear regression). Statistically significant values ($P < 0.05$) are in bold. Model I: unadjusted model; Model II: adjusted for age, BMI, fasting plasma glucose; Model III: adjusted for age, BMI, fasting blood glucose, systolic blood pressure, diastolic blood pressure, subcutaneous fat, visceral fat, and liver fat deposition. Abbreviation: SE, standard error

tail. RC exhibited a positive correlation with total IPFD across all models (Model I: R^2=0.056, P<0.001; Model II: R^2=0.081, P<0.001; Model III: R^2=0.155, P<0.001). RC also showed a significant correlation with fat deposition in the head of the pancreas in all models (Model I: R^2=0.042, P<0.001; Model II: R^2=0.055, P<0.001; Model III: R^2=0.124, P=0.003), and with fat deposition in the pancreatic body (Model I: R^2=0.045, P<0.001; Model II: R^2=0.067, P<0.001; Model III: R^2=0.102, P=0.001) and tail (Model I: R^2=0.037, P<0.001; Model II: R^2=0.067, P<0.001; Model III: R^2=0.146, P=0.005). In contrast, TG showed no significant correlation with total IPFD or with fat deposition in the head, body, or tail of the pancreas in the final adjusted model. HDL-C showed no significant correlation with total IPFD or with fat deposition in the head or body of the pancreas in any of the models. A negative correlation between HDL-C and fat deposition in the pancreatic tail was observed in Model I, but this was not evident in the other two models. Similarly, LDL-C showed no significant correlation with total IPFD, or with fat deposition in the pancreatic head, body, or tail in any model. Consistently, the TC/HDL-C and TG/HDL-C ratios demonstrated no significant links to total IPFD or fat deposition in the pancreatic head, body, or tail in the final adjusted model (Table 3).

Discussion

This extensive QCT study on IPFD included over a thousand participants, adjusted for eight covariates, and included gender-specific analyses. Lipid panel correlations with intra-pancreatic fat deposition were more pronounced in women than in men. In men, relationships with intra-pancreatic fat deposition were notable only in the pancreatic tail with TC, TG, and TG/HDL-C, whereas in women, both TC and RC were positively correlated with IPFD, with RC more closely related to IPFD. There were no notable associations involving TG, HDL-C, LDL-C, or the TC/HDL-C ratio in either gender. Notably, the relationships between lipid panel parameters and fat deposition in different pancreatic regions were not consistent, regardless of sex. In a cross-sectional study involving 348 individuals, Skudder-Hill et al. [16] used MRI to measure IPFD and indicated that the association between lipid panel parameters and fat deposition in different intra-pancreatic regions was inconsistent. This variability in the relationships between lipid panel parameters and regional intra-pancreatic fat deposition may stem from the heterogeneous distribution of intra-pancreatic fat deposition, which includes both intralobular fat (such as in endocrine and acinar cells) and interlobular fat [22]. By further emphasizing this point, Begovatz et al. [25] observed that intra-pancreatic fat deposition in certain regions of the pancreas produced an uneven distribution of adipose tissue infiltration.

In the pooled data, RC emerged as the strongest predictor of IPFD in women. For RC with total IPFD, the final adjusted R^2 was 0.155; with intra-pancreatic head fat deposition, the final adjusted R^2 was 0.124; with intra-pancreatic body fat deposition, the final adjusted R^2 was 0.102; and with intra-pancreatic tail fat deposition, the final adjusted R^2 was 0.146. The positive correlation between RC and IPFD was first corroborated in a cross-sectional analysis by Skudder-Hill et al. [16], where the participants had an average age of 50 years, which was very similar to this study population; however, there was no differentiation in the population by sex, and the present study fills this gap. Therefore, insulin resistance may have a mediating role in the link between RC and IPFD, as demonstrated by Vargas-Vázquez et al. [26] in a cross-sectional analysis involving 16,201 nondiabetic participants, in which RC was shown to influence cardiovascular mortality by enhancing systemic insulin sensitivity. Furthermore, Patel et al. [18] found in a case–control analysis that insulin resistance was positively correlated with intra-pancreatic fat deposition, leading to the hypothesis that remnant cholesterol may influence intra-pancreatic fat deposition by affecting insulin resistance. In males, however, there was no significant correlation between remnant cholesterol and intra-pancreatic fat deposition, and the underlying causes of this sex difference remain unknown. This may be due to hormonal differences, but the underlying mechanisms need further research.

There is significant controversy surrounding the association between TC and IPFD. This study revealed a positive link between TC and IPFD, in line with with the findings of the cross-sectional study by Dong Zhi et al. [11], which involved 83 participants. However, Dong Zhi et al.'s study focused on individuals with impaired glucose tolerance or type 2 diabetes, whereas the research in this study expanded to a broader population. In a separate investigation by Singhet et al. [13], the association between IPFD and lipid metabolism markers was examined in healthy individuals without obesity, and no notable correlation between the TC level and IPFD was found. Notably, that study involved only 23 participants. Additionally, Skudder-Hill et al. [16], in a cross-sectional analysis comprising 348 participants, reported no significant association between TC and IPFD, but there was no adjustment for visceral fat, which has been shown to be strongly correlated with IPFD [27]. The present study is more comprehensive than the aforementioned, both in terms of participant numbers and adjustments for confounding factors.

In addition, this study revealed a positive correlation of TG with intra-pancreatic tail fat deposition in men. Skudder-Hill et al. [16] identified a positive correlation linking TG and IPFD; Singhet al. [10], in a meta-study involving

Table 3 Correlations between serum lipid profiles, serum lipoprotein ratios, and the deposition //of fat in the pancreas of females

Component/Model	Total				Head				Body				Tail			
	R2	β	SE	p	R2	β	SE	p	R2	β	SE	p	R2	β	SE	p
Triglycerides																
Model I	0.033	0.506	0.142	**< 0.001**	0.028	0.541	0.167	**0.001**	0.021	0.513	0.184	**0.006**	0.027	0.463	0.145	**0.002**
Model II	0.048	0.400	0.151	**0.009**	0.034	0.502	0.179	**0.005**	0.036	0.360	0.196	0.067	0.046	0.340	0.155	**0.029**
Model III	0.125	0.153	0.153	0.319	0.098	0.223	0.182	0.220	0.075	0.147	0.203	0.468	0.128	0.087	0.156	0.577
Total cholesterol																
Model I	0.030	0.724	0.214	**0.001**	0.026	0.792	0.252	**0.002**	0.032	0.962	0.276	**0.001**	0.010	0.418	0.221	0.059
Model II	0.049	0.617	0.226	**0.007**	0.033	0.728	0.266	**0.007**	0.051	0.887	0.290	**0.002**	0.037	0.237	0.232	0.306
Model III	0.145	0.664	0.216	**0.002**	0.117	0.777	0.256	**0.003**	0.100	0.929	0.285	**0.001**	0.131	0.285	0.222	0.199
Remnant cholesterol																
Model I	0.056	1.019	0.217	**< 0.001**	0.042	1.039	0.257	**< 0.001**	0.045	1.173	0.281	**< 0.001**	0.037	0.845	0.224	**< 0.001**
Model II	0.081	0.982	0.217	**< 0.001**	0.055	1.029	0.258	**< 0.001**	0.067	1.112	0.281	**< 0.001**	0.067	0.806	0.223	**< 0.001**
Model III	0.155	0.778	0.216	**< 0.001**	0.124	0.767	0.259	**0.003**	0.102	0.951	0.282	**0.001**	0.146	0.607	0.218	**0.005**
High-density lipoprotein cholesterol																
Model I	0.008	-0.925	0.542	0.089	0.003	-0.704	0.636	0.269	0.003	-0.716	0.699	0.307	0.127	-1.354	0.500	**0.014**
Model II	0.033	-0.652	0.548	0.235	0.015	-0.550	0.647	0.396	0.028	-0.312	0.707	0.660	0.044	-1.093	0.556	0.050
Model III	0.123	0.099	0.540	0.855	0.095	0.317	0.642	0.622	0.074	0.352	0.714	0.622	0.128	-0.373	0.549	0.498
Low-density lipoprotein cholesterol																
Model I	< 0.001	-0.071	0.212	0.739	< 0.001	-0.040	0.248	0.873	< 0.001	-0.037	0.272	0.892	0.001	-0.135	0.216	0.531
Model II	0.033	-0.266	0.221	0.229	0.015	-0.202	0.261	0.441	0.029	-0.220	0.285	0.442	0.041	-0.377	0.225	0.094
Model III	0.123	-0.128	0.213	0.549	0.095	-0.047	0.253	0.852	0.074	-0.098	0.282	0.729	0.130	-0.238	0.030	0.272
Triglycerides/High-density lipoprotein cholesterol																
Model I	0.023	0.266	0.090	**0.003**	0.019	0.281	0.106	**0.008**	0.014	0.269	0.116	**0.021**	0.019	0.249	0.092	**0.007**
Model II	0.042	0.209	0.094	**0.026**	0.028	0.260	0.111	**0.020**	0.033	0.181	0.121	0.136	0.043	0.187	0.096	0.052
Model III	0.124	0.078	0.095	0.403	0.103	0.100	0.113	0.373	0.071	0.081	0.028	0.518	0.135	0.056	0.096	0.559
Total Cholesterol/High-density lipoprotein cholesterol																
Model I	0.025	0.399	0.129	**0.002**	0.018	0.398	0.151	**0.009**	0.022	0.479	0.166	**0.004**	0.016	0.319	0.132	**0.016**
Model II	0.045	0.326	0.131	**0.014**	0.027	0.352	0.155	**0.024**	0.041	0.396	0.170	**0.020**	0.041	0.230	0.134	0.087
Model III	0.130	0.218	0.130	0.093	0.107	0.226	0.155	0.145	0.079	0.311	0.172	0.071	0.136	0.119	0.132	0.369

Note: Data are presented as R2 values, unstandardized β coefficients, standard errors, and *P* values (from linear regression). Statistically significant values ($P < 0.05$) are in bold. Model I: unadjusted model; Model II: adjusted for age, BMI, fasting plasma glucose; Model III: adjusted for age, BMI, fasting blood glucose, systolic blood pressure, diastolic blood pressure, subcutaneous fat, visceral fat, and liver fat deposition. Abbreviation: SE, standard error

17 parameters and 11,967 participants, reported a positive correlation between TG and IPFD. Hypertriglyceridemia was the most common metabolic abnormality and was strongly associated with the state of insulin resistance. Therefore, TG, similar to RC, may affect intrapancreatic fat deposition by influencing insulin resistance [28, 29]. Notably, the present study was stratified by gender, showing that triglycerides were related to IPFD in men but not in women. This suggests that the inconsistency in results between sexes may be due to metabolic differences between the sexes.

The TG/HDL-C ratio was also observed to have a positive correlation with fat deposition in the pancreatic tail in men. Notably, in Singh et al.'s study on a healthy non-obese population, no association between the two was reported, whereas a positive correlation in a population with previously diagnosed with acute pancreatitis was reported. Research by Singh et al. suggested that the association of the TG/HDL-C ratio with intra-pancreatic fat deposition varied across different populations [13]. The study is the initial study in which a positive correlation was found linking the TG/HDL-C ratio and fat deposition in the tail of the pancreas in males. This may be mediated by insulin resistance, although further experiments are needed to verify this [17].

Study strengths and limitations

This research represents the first comprehensive exploration of associations among serum lipid profiles, lipoprotein ratios, and IPFD, with an emphasis on sex stratification. QCT was used to measure pancreatic fat. Histopathological examination has long been regarded as the benchmark for quantifying pancreatic fat. However, because of its deep-seated pancreatic location, biopsy poses significant health risks and has a high risk of sampling errors, making it unsuitable for routine clinical application. Among various imaging modalities, MRI is currently recognized as the most accurate and widely used method. The recently developed MRI mDIXON Quant offers several advantages, such as being non-invasive, fast, and capable of single-shot imaging, and has demonstrated good consistency when compared to biopsy and phantom models [30, 31]. However, its lengthy process and high expense restrict its broader clinical application Yao Wenjun et al. [32] conducted a Pearson analysis that showed a strong link between QCT and the MRI mDIXON Quant for quantifying pancreatic fat content, with $r=0.805$ ($P<0.0001$). Some limitations must be acknowledged: the cross-sectional design prevents establishing causality, and the predominantly Asian sample population could restrict the generalization of the findings across diverse populations. Therefore, cohort studies with diverse populations are needed to validate these findings. In this study, individuals taking weight- and metabolism-modifying medications and those who had lost weight through diet or exercise were excluded, potentially restricting the applicability of the findings. Additionally, previous research has demonstrated that individuals having type 2 diabetes exhibit reduced pancreatic density compared to controls [33, 34], and because a lower density correlates with increased fat content, this confounding factor is significant for this study. However, because the population in this study consisted of healthy individuals undergoing routine checkups, diabetes history data were not available.

Conclusion

In this study, sex differences in the association between serum lipids, lipoprotein ratios, and IPFD were clearly observed. In males, the correlations between serum lipids, lipoprotein ratios, and IPFD were limited to the pancreatic tail, involving TC and TG levels and the TG/HDL-C ratio, but these correlations were relatively weak. In females, RC and TC levels were associated with IPFD, and the relationship with RC was more pronounced. This finding highlighted the important role of RC in female IPFD, indicating RC may serve as a new marker in early detection and prevention of female IPFD.

Acknowledgements
The authors extend their gratitude for all the financial support received and to all the team members and contributors who assisted with this study. We acknowledge LetPub (www.letpub.com.cn) for providing linguistic support in preparing this manuscript.

Author contributions
Ting Ran and Yanni Wang contributed equally to this work. (A): Conception and design: Jing Zheng, Xia Du; (B): Data collection: Yanni Wang, Fengxi Yuan, Ruoyi Liu; (C) Data analysis: Ting Ran, Yanni Wang; (D): Drafted the manuscript: Ting Ran; (E) Revision of the manuscript: Jing Zheng, Xia Du, Miao Zhang, Juan He; (F) Final approval of manuscript: All authors.

Funding
This study was funded by the National Natural Science Foundation of China (grant no. 82260175), the Guizhou Provincial Science and Technology Department Project (grant no. qian ke he jichu-ZK [2024] yiban188), the National Natural Science Foundation of Guizhou Medical University (grant no. 21NSFCP06), and the Provincial Key Medical Discipline Construction Project of the Health Commission of Guizhou Province from 2023 to 2024 (grant no. qian wei jian han [2023] no. 2).

Data availability
No datasets were generated or analysed during the current study.

Declarations

Ethical statement
The need for ethical approval was waived by the local Ethics Committee at Guizhou Medical University due to the study's retrospective nature.

Competing interests
The authors declare that they have no potential conflicts of interest with respect to the research, authorship, and/or publication of this article.

Received: 22 August 2024 / Accepted: 31 October 2024
Published online: 02 January 2025

References

1. Petrov MS, Taylor R. Intra-pancreatic fat deposition: bringing hidden fat to the fore. Nat Rev Gastroenterol Hepatol. 2022;19(3):153–68.
2. Singh RG, Yoon HD, Wu LM, Lu J, Plank LD, Petrov MS. Ectopic fat accumulation in the pancreas and its clinical relevance: a systematic review, meta-analysis, and meta-regression. Metabolism. 2017;69:1–13.
3. Petrov MS. Harnessing Analytic Morphomics for early detection of pancreatic Cancer. Pancreas. 2018;47(9):1051–4.
4. Petrov MS, Yadav D. Global epidemiology and holistic prevention of pancreatitis. Nat Rev Gastroenterol Hepatol. 2019;16(3):175–84.
5. Cho J, Scragg R, Petrov MS. Risk of mortality and hospitalization after Post-pancreatitis Diabetes Mellitus vs type 2 diabetes Mellitus: a Population-based Matched Cohort Study. Am J Gastroenterol. 2019;114(5):804–12.
6. Lee MS, Lee JS, Kim BS, Kim DR, Kang KS. Quantitative analysis of pancreatic Fat in children with Obesity Using Magnetic Resonance Imaging and Ultrasonography. Pediatr Gastroenterol Hepatol Nutr. 2021;24(6):555–63.
7. Kato S, Iwasaki A, Kurita Y, Arimoto J, Yamamoto T, Hasegawa S, et al. Three-dimensional analysis of pancreatic fat by fat-water magnetic resonance imaging provides detailed characterization of pancreatic steatosis with improved reproducibility. PLoS ONE. 2019;14(12):e0224921.
8. Idilman IS, Tuzun A, Savas B, Elhan AH, Celik A, Idilman R, et al. Quantification of liver, pancreas, kidney, and vertebral body MRI-PDFF in non-alcoholic fatty liver disease. Abdom Imaging. 2015;40(6):1512–9.
9. Saisho Y, Butler AE, Meier JJ, Monchamp T, Allen-Auerbach M, Rizza RA, et al. Pancreas volumes in humans from birth to age one hundred taking into account sex, obesity, and presence of type-2 diabetes. Clin Anat. 2007;20(8):933–42.
10. Singh RG, Yoon HD, Poppitt SD, Plank LD, Petrov MS. Ectopic fat accumulation in the pancreas and its biomarkers: a systematic review and meta-analysis. Diabetes Metab Res Rev. 2017;33(8).
11. Dong Z, Luo Y, Cai H, Zhang Z, Peng Z, Jiang M, et al. Noninvasive fat quantification of the liver and pancreas may provide potential biomarkers of impaired glucose tolerance and type 2 diabetes. Med (Baltim). 2016;95(23):e3858.
12. Honka H, Hannukainen JC, Tarkia M, Karlsson H, Saunavaara V, Salminen P, et al. Pancreatic metabolism, blood flow, and β-cell function in obese humans. J Clin Endocrinol Metab. 2014;99(6):E981–990.
13. Singh RG, Nguyen NN, Cervantes A, Cho J, Petrov MS. Serum lipid profile as a biomarker of intra-pancreatic fat deposition: a nested cross-sectional study. Nutr Metab Cardiovasc Dis. 2019;29(9):956–64.
14. Oliveri A, Rebernick RJ, Kuppa A, Pant A, Chen Y, Du X, et al. Comprehensive genetic study of the insulin resistance marker TG:HDL-C in the UK Biobank. Nat Genet. 2024;56(2):212–21.
15. Targher G, Rossi AP, Zamboni GA, Fantin F, Antonioli A, Corzato F, et al. Pancreatic fat accumulation and its relationship with liver fat content and other fat depots in obese individuals. J Endocrinol Invest. 2012;35(8):748–53.
16. Skudder-Hill L, Sequeira-Bisson IR, Ko J, Cho J, Poppitt SD, Petrov MS. Remnant cholesterol, but not low-density lipoprotein cholesterol, is associated with intra-pancreatic fat deposition. Diabetes Obes Metab. 2023;25(11):3337–46.
17. Brehm A, Pfeiler G, Pacini G, Vierhapper H, Roden M. Relationship between serum lipoprotein ratios and insulin resistance in obesity. Clin Chem. 2004;50(12):2316–22.
18. Patel NS, Peterson MR, Lin GY, Feldstein A, Schnabl B et al. Bettenc. t R,. Insulin Resistance Increases MRI-Estimated Pancreatic Fat in Nonalcoholic Fatty Liver Disease and Normal Controls. Gastroenterol Res Pract. 2013;2013:498296.
19. Nadarajah C, Fananapazir G, Cui E, Gichoya J, Thayalan N, Asare-Sawiri M, et al. Association of pancreatic fat content with type II diabetes mellitus. Clin Radiol. 2020;75(1):51–6.
20. Triay Bagur A, Aljabar P, Ridgway GR, Brady M, Bulte DP. Pancreas MRI segmentation into Head, body, and tail enables Regional quantitative analysis of Heterogeneous Disease. J Magn Reson Imaging. 2022;56(4):997–1008.
21. Cheng X, Blake GM, Brown JK, Guo Z, Zhou J, Wang F, et al. The measurement of liver fat from single-energy quantitative computed tomography scans. Quant Imaging Med Surg. 2017;7(3):281–91.
22. Yao WJ, Guo Z, Wang L, Li K, Saba L, Guglielmi G, et al. Pancreas fat quantification with quantitative CT: an MRI correlation analysis. Clin Radiol. 2020;75(5):397.e1-397.e6.
23. Guo Z, Blake GM, Li K, Liang W, Zhang W, Zhang Y, et al. Liver Fat Content Measurement with quantitative CT validated against MRI Proton Density Fat Fraction: a prospective study of 400 healthy volunteers. Radiology. 2020;294(1):89–97.
24. Chait A, Ginsberg HN, Vaisar T, Heinecke JW, Goldberg IJ, Bornfeldt KE. Remnants of the Triglyceride-Rich Lipoproteins, diabetes, and Cardiovascular Disease. Diabetes. 2020;69(4):508–16.
25. Begovatz P, Koliaki C, Weber K, Strassburger K, Nowotny B, Nowotny P, et al. Pancreatic adipose tissue infiltration, parenchymal steatosis and beta cell function in humans. Diabetologia. 2015;58(7):1646–55.
26. Vargas-Vázquez A, Fermín-Martínez CA, Antonio-Villa NE, Fernández-Chirino L, Ramírez-García D, Dávila-López G et al. Insulin resistance potentiates the effect of remnant cholesterol on cardiovascular mortality in individuals without diabetes. Atherosclerosis. 2024;117508.
27. Staaf J, Labmayr V, Paulmichl K, Manell H, Cen J, Ciba I, et al. Pancreatic Fat is Associated with metabolic syndrome and visceral Fat but not Beta-cell function or body Mass Index in Pediatric obesity. Pancreas. 2017;46(3):358–65.
28. Lamarche B, Després JP, Pouliot MC, Prud'homme D, Moorjani S, Lupien PJ, et al. Metabolic heterogeneity associated with high plasma triglyceride or low HDL cholesterol levels in men. Arterioscler Thromb. 1993;13(1):33–40.
29. Reaven GM, Syndrome X. 6 years later. J Intern Med Suppl. 1994;736:13–22.
30. Sepe PS, Ohri A, Sanaka S, Berzin TM, Sekhon S, Bennett G, et al. A prospective evaluation of fatty pancreas by using EUS. Gastrointest Endosc. 2011;73(5):987–93.
31. Smereczyński A, Kołaczyk K. Is a fatty pancreas a banal lesion? J Ultrason. 2016;16(66):273–80.
32. Yao Wenjun. (2020). Feasibility and Value of Studying Pancreatic Fat Content in Healthy Individuals Based on MR Proton Density Fat Fraction and Quantitative CT Technology (Doctoral Dissertation, Anhui Medical University). Doctoral.dissertation.https://link.cnki.net/doi/10.26921/d.cnki.ganyu.2020.000013
33. Alexandre-Heymann L, Barral M, Dohan A, Larger E. Patients with type 2 diabetes present with multiple anomalies of the pancreatic arterial tree on abdominal computed tomography: comparison between patients with type 2 diabetes and a matched control group. Cardiovasc Diabetol. 2020;19(1):122.
34. Lim S, Bae JH, Chun EJ, Kim H, Kim SY, Kim KM, et al. Differences in pancreatic volume, fat content, and fat density measured by multidetector-row computed tomography according to the duration of diabetes. Acta Diabetol. 2014;51(5):739–48.

Publisher's note